https://doi.org/10.5194/essd-2024-452
Preprint. Discussion started: 28 October 2024

Open Access Earth System Science Data Discussions

Exploring the CO_2 fugacity along the east coast of South America aboard the schooner *Tara*

Léa Olivier[1,2], Jacqueline Boutin[2], Gilles Reverdin[2], Christopher Hunt[3], Thomas Linkowski[4], Alison Chase[5,6], Nils Haentjens[6], Pedro C. Junger[7,8*], Stéphane Pesant[9], & Douglas Vandemark[3]

[1]Alfred Wegener Institute, Helmholtz Centre for Polar and Marine Research, Bremerhaven, Germany
[2]LOCEAN-IPSL, Sorbonne Université-CNRS-IRD-MNHN, Paris, France
[3]OPAL, EOS, University of New Hampshire, Durham, New Hampshire, USA
[4]Fondation Tara Ocean
[5]Applied Physics Laboratory, University of Washington, Seattle, Washington
[6]School of Marine Sciences, University of Maine, Orono, Maine
[7]Department of Hydrobiology, Universidade Federal de São Carlos (UFSCar), São Carlos, SP 13565-905, Brazil
[8]Programa de Pós-Graduação em Ecologia e Recursos Naturais, Centro de Ciências Biológicas e da Saúde, Universidade Federal de São Carlos (UFSCar), São Carlos, SP 13565-905, Brazil
[9]European Molecular Biology Laboratory, European Bioinformatics Institute, Wellcome Genome Campus, Hinxton, Cambridge CB10 1SD, United Kingdom
*Present address: Institut de Biologie de l'École Normale Supérieure (IBENS), École Normale Supérieure, CNRS, INSERM, PSL Université Paris, Paris 75005, France.

Correspondence to: Léa Olivier (lea.olivier@awi.de)

Abstract. The air-sea CO_2 flux in the coastal ocean is a key component of the global carbon budget. However, due to the scarcity of data, the many sources and sinks of carbon and their complex interactions in these waters remain poorly understood. In 2021, the *Tara* schooner collected 14,000 km of CO_2 fugacity (fCO_2) measurements along the coast of South America, including in the Amazon River-Ocean continuum (https://doi.org/10.5281/zenodo.13790065, Olivier et al., 2024a). The interactions between the Amazon River and its oceanic plume are complex, and under a combined influence of many processes such as tides and bathymetry. Downstream of the Amazon River plume, the fCO_2 is low compared with that of the atmosphere, reaching a minimum of 42 µatm. In the river, fCO_2 reaches up to 3000 µatm. South of the estuary, the waters of the North Brazil Current have a fCO_2 exceeding 400 µatm. Along the Brazil Current, fCO_2 is around 400 µatm and decreases, as does temperature, as the schooner sails away from the equator. Nevertheless, in all the data collected in this coastal environment, salinity varies greatly, and therefore describes best the variability of fCO_2. Despite the strong variability and uncertainties in the data, comparison with discrete samples of other carbonate parameters shows that the mean differences (2 µatm) are within the range of uncertainties related to the chemical formula used for the comparison. This data set helps to fill the gap in our knowledge of the behavior of fCO_2 in the under-sampled region of the Brazilian coast.

https://doi.org/10.5194/essd-2024-452
Preprint. Discussion started: 28 October 2024

1 Introduction

The global ocean is a sink that absorbs 26% of the anthropogenic carbon dioxide (CO_2) emitted into the atmosphere by the burning of fossil fuels and land use change (Friedlingstein et al., 2023). While the ocean participates in mitigating the effects of climate change by storing both heat and CO_2, it is also subject to profound changes such as ocean warming and acidification. Coastal and marginal oceans play a pivotal role in the global carbon cycle by connecting terrestrial, oceanic and atmospheric carbon reservoirs. The air-sea CO_2 flux varies spatially over the world's oceans, and some of the strongest gradients are found in the coastal regions (Landschützer et al., 2020). These regions present much higher temporal and spatial variability compared to the open ocean (Borges, 2005; Cai et al., 2006; Laruelle et al., 2014; Roobaert et al., 2019). Recent studies estimate that the uptake of CO_2 per unit area is even greater over continental shelf seas than over the open ocean due to the contribution of the arctic shelves and the impact of rivers (Chen et al., 2013; Laruelle et al., 2014; Roobaert et al., 2019). Despite the fact that coastal waters play a major role in the livelihood of humans, and are strongly affected by human activities, our understanding of these waters is strongly limited by the low number of observations (Bauer et al., 2013).

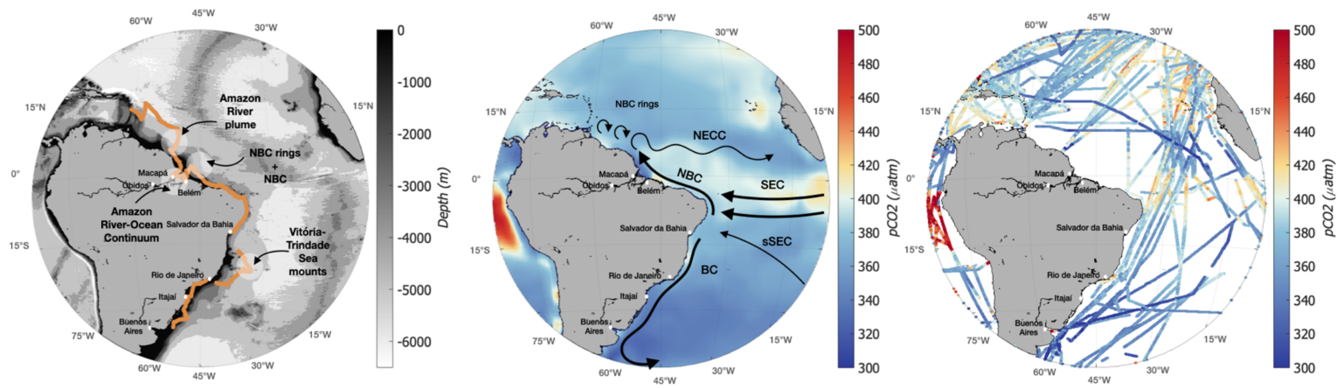

Figure 1: a) Bathymetry of the Atlantic Ocean (ETOPO2v2) and journey of the schooner *Tara* (orange line). b) 1998-2015 September climatology of the partial pressure of CO_2 (pCO_2, Landschützer et al., 2020), the black arrows represent some of the main surface geostrophic currents in boreal fall. c) pCO_2 along the ship trajectories in August-September-October (SOCAT, data from 1957 to 2022). NBC: North Brazil Current, NECC: North Equatorial Counter Current, SEC: South Equatorial Current, sSEC: southern branch of the SEC, BC: Brazil Current.

While the coastal and marginal seas of the mid and northern latitudes are sinks of CO_2 with regards to the atmosphere, the tropical coastal oceans act as sources (Cai et al., 2006; Laruelle et al., 2014; Takahashi et al., 2002). There are several reasons for this, including the reduced solubility of CO_2 at high temperatures, and the upwelling of deep waters rich in dissolved inorganic carbon (DIC) in the equatorial upwelling and along the coast. This has also been observed on regional studies, and one region presenting a strong and heterogeneous signal is the western tropical Atlantic coastal ocean (Lefèvre et al., 2017; Lefévre et al., 2010; Olivier et al., 2022).

https://doi.org/10.5194/essd-2024-452
Preprint. Discussion started: 28 October 2024

One example is the Amazon river-ocean continuum (AROC). It represents one of the greatest environmental gradients on land and ocean in the world. The Amazon River system discharge is unique in the global ocean. It contributes as much freshwater as the next seven largest rivers combined, accounting for 20% of the global riverine freshwater input to the ocean (Dai and Trenberth, 2002). The resulting Amazon River plume (ARP) spreads across up to 1.3 million km² of the tropical Atlantic Ocean and creates a significant CO_2 sink relative to the atmosphere, primarily driven by strong biological drawdown (Cooley et al., 2007; Körtzinger, 2003; Subramaniam et al., 2008). Opposing this, the Amazon River outgasses nearly as much CO_2 as the rainforest sequesters on an annual basis. The main source of CO_2 in the river comes from the breakdown of young organic carbon from the land by microbes (Mayorga et al., 2005; Ward et al., 2013, 2015). The lower Amazon River (from Óbidos to the river mouth) releases an amount of CO_2 slightly higher (0.02 Pg C yr^{-1}, Sawakuchi et al., 2017) than the uptake by the ARP in the Atlantic Ocean (0.014 Pg C yr^{-1}, Körtzinger, 2003). Sawakuchi et al. (2017) demonstrated the importance of quantifying CO_2 fluxes in the lower Amazon by adding the Óbidos-Macapá section to the Amazon River budget. On the other hand, oceanographic studies, carried out in particular during the ANACONDAS (Mu et al., 2021) and Camadas Finas III (Araujo et al., 2017) campaigns, have shown the extent of CO_2 undersaturation in the ARP. However, the link between these two systems is little known, if at all (Sawakuchi et al., 2017; Ward et al., 2017). Chen et al. (2013) extensively studied the CO_2 in the world's coastal seas by evaluating the air-sea exchanges of CO_2 in 165 estuaries, but no data were available in the Amazon estuary, despite being arguably one with the strongest impact. Since then, only discrete samples of DIC and total alkalinity (TA) have been taken at the mouth of the Pará-Tocantins River system, near the town of Belém (Araujo et al., 2017).

While the data gap in the open ocean has slowly started to be filled up by the development of the Argo program, it is not the case for biogeochemical measurement on the shelves and continental margins. This is also not the case for the continuous fugacity of CO_2 (fCO_2) measurements carried out on ships. Despite recent sampling, as reported by the Surface Ocean CO_2 Atlas (SOCAT) database (Bakker et al., 2016), the continental margins off Brazil are lacking in data, and even more notably when considering a particular season, such as from August to November (Fig. 1c). The number of data being added to SOCAT is also decreasing significantly since 2017 (Friedlingstein et al., 2023). Recently, sailboats have provided interesting opportunities to measure CO_2 in conditions different from traditional research vessels, as highlighted by the contribution of data from racing sailboats (Landschützer et al., 2023).

Here, we present a new fCO_2 data set, acquired on the research schooner *Tara*. This is the first time that a sailboat has been equipped with a fCO_2 equilibrator-system, which is more accurate than the membrane system used on racing yachts, but larger and more maintenance-intensive. One of the special features of the missions aboard *Tara* is the combination of physical, biogeochemical, and biological oceanography to provide comprehensive knowledge of the ocean (Bork et al., 2015; Pesant et al., 2015). Tara missions are unique in that they are continuous for a multi-year duration, with scientists and sailors taking turns on-board. This novel dataset presents 14,000 km of fCO_2 data mostly along the coasts of South America, from August to December 2021, for the first-time sampling the AROC multiple times. It also includes measurements in the ARP and in

https://doi.org/10.5194/essd-2024-452
Preprint. Discussion started: 28 October 2024

different areas off Brazil: in the North Brazil Current (NBC), the Brazil Current, the Guanabara Bay (Rio de Janeiro), the Vitória-Trindade Sea mounts and the shelves of South Brazil, filling some of the gaps in the current data.

The primary objective of this study is to present the fCO_2 dataset acquired by *Tara*, and shed light on some of the lesser studied areas of the Amazon River. Section 2 provides a detailed description of the fCO_2 measurement system, the challenges encountered during its installation on the schooner, the solutions implemented, and the validation of the dataset. Section 3 illustrates the dataset, first encompassing the whole transect and then focusing on the case study of the river-ocean continuum. Section 4 discusses possible uses of the data and the performance of the system.

2 Instruments and methodology

2.1. Mission Microbiomes AtlantECO

For two years, the schooner *Tara* sailed 70,000 kilometers across the South Atlantic Ocean to study the ocean microbiome and its interactions with climate and pollution. The 36 m long schooner is equipped with numerous scientific equipment operated by a team of four to six scientists and six sailors consistently on board. During the first part of the Mission Microbiomes AtlantECO, the schooner sampled the entire east coast of South America, from August to end of November 2021 (Fig. 1a). The dataset presented in this study focuses on the underway data collected during the legs 5, 6, 7, 8 and 9 of the Mission Microbiome. Leg 5 started on 18 August from Fort-de-France (Martinique, France) and ended in Macapá (Brazil) on 9 September. Leg 6 left Macapá on 12 September to reach Belém (Brazil) on 17vSeptember. Leg 7 started on 24 September and ended in Salvador da Bahia (Brazil) on 9 October. After a stopover of a week in Salvador da Bahia, the schooner left for leg 8 on 17 October and arrived in Rio de Janeiro (Brazil) on 3 November. Leg 9 started from Rio on 11 November, and included a stop in Santos (Brazil) from 11 November to 13 November and a stop in Itajaí (Brazil) from 15 November to 19 November ending in Buenos-Aires (Argentina) on 27 November. The dataset stops on 25 November, as the authorization to sample in the exclusive economic zone of Uruguay was not obtained.

2.2. Underway fCO_2-system

An equilibrator-based system from the university of New Hampshire (Vandemark et al., 2011) was installed on *Tara* in July 2021. It monitored continuously the near-surface ocean fCO_2 (Fig. 2). Currently, an equilibrator-based fCO_2 system is the most reliable and accurate instrument to measure the in-situ fCO_2 in seawater. It is able to capture the fine scale variability of oceanic fCO_2 by responding quickly to fCO_2 changes in seawater. The exchange time for the water in the equilibrator is between 30 and 45 seconds, depending on flow rate (Pierrot et al., 2009). Unlike a traditional research vessel (RV), space and time for

https://doi.org/10.5194/essd-2024-452
Preprint. Discussion started: 28 October 2024

maintenance are limited on board the schooner. The continuous water line is used by 9 instruments, stored under in the fore hold, and in a small laboratory of a few square meters. The installation of the CO_2 system required some compromises chosen with help from the sailors and engineers on board, to fit with the schooner constraints and to limit the loss in measurement accuracy (originally of less than 2 µatm). We will detail the modifications in the setup of the fCO_2 system, and then discuss the accuracy of the data obtained, before illustrating the large variability of the sampled area.

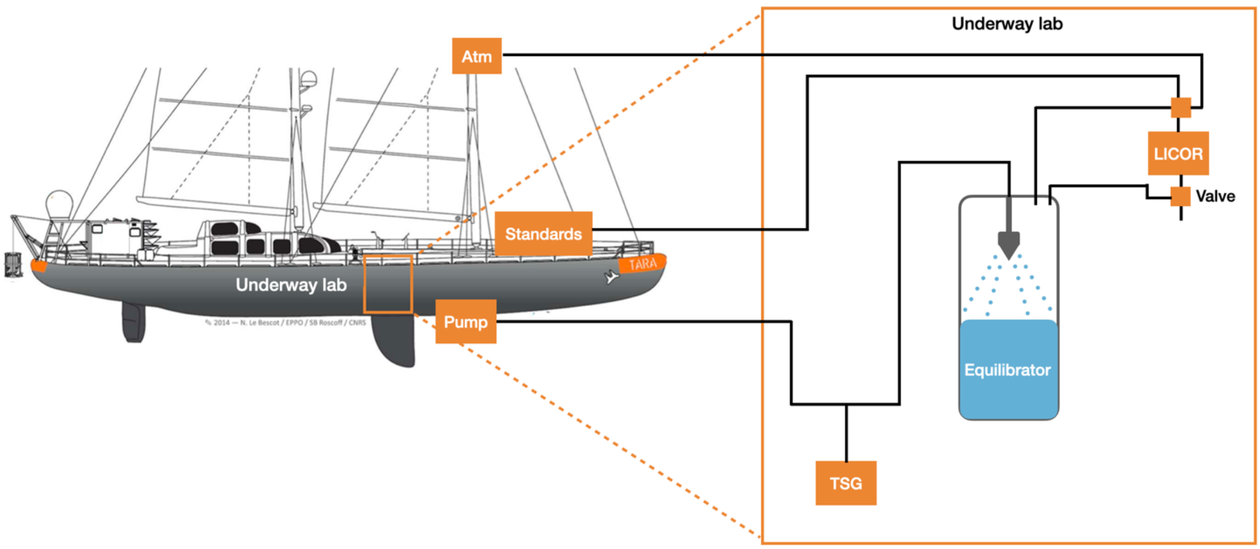

Figure 2: Schematic of the underway laboratory and fCO_2 system onboard the schooner *Tara*, adapted from (Pesant et al., 2015).

Seawater enters through the hull at less than 1.5 m depth where a Sea Bird Electronics (SBE) 38 temperature sensor is located for an accurate measurement of sea surface temperature (SST). It then enters a debubbler to remove most of the bubbles that can be caused by such shallow water intake, especially in rough seas. The seawater circuit is then split into two to feed the many underway instruments. One branch flows first through a thermosalinograph (TSG, SBE 45) to accurately measure temperature and salinity (temperature accuracy of ± 0.002 °C, conductivity accuracy of ± 0.0003 S m^{-1}). The other branch first flows into the equilibrator of the fCO_2 system after less than 5 m of tubing, at a rate of 2-6 L min^{-1}. We make the hypothesis that at this high flow rate and short path, the temperature is similar in the equilibrator and in the TSG, as both instruments are first in their respective water circuit and at a similar distance from the split. We suspect that this choice introduces less uncertainty than using directly SST (action recommended for missing equilibrator temperature data, Pierrot et al., 2009), although we do not have the data to fully validate this hypothesis. Fortunately, the sailboat is small compared to an open ocean RV, so the pipe length from the hull to the underway instruments is considerably smaller and the temperature difference between the hull sensor and the TSG is small (always below 0.5 °C averaging 0.07°C).

https://doi.org/10.5194/essd-2024-452
Preprint. Discussion started: 28 October 2024

Open Access Earth System Science Data Discussions

The fCO_2 system uses a shower spray air–sea equilibrator described by (Dickson, 2007; Vandemark et al., 2011). A closed loop of air flows through the equilibrator where the air-water exchanges happen, the equilibrated air is then dried and sent to the CO_2 analyzer, a LICOR LI-840A. It detects the molar fraction of CO_2 (xCO_2) in dry air by infrared detection, from which fCO_2 is computed following Henry's law (Pierrot et al., 2009, detailled in Annex). Ideally, the computation requires the pressure inside the equilibrator. The equilibrator was not equipped with a pressure sensor, but was designed to be at atmospheric pressure. Atmospheric pressure was measured by a Vaisala Barometer PTB100 with an accuracy of ± 0.3 hPa at 20°C at the rear of the ship. A temperature correction to the seawater fCO_2 data is applied based on the difference between the temperature sensor in the hull and the TSG.

Through a system of valves, four circuits are operated, one for the air equilibrated with seawater, one for each of the two reference gases, and one for the atmospheric air. The atmospheric air intake is located on the first cross tree of the schooner front mast (~ 10 m). The two 20 L reference gases tanks of 0 ppm and 502.3 ppm are stored on the front deck.

The number of different calibration gases was reduced from 4 (on a traditional RV) to 2 (as done on racing sailboats, Landschützer et al., 2023). The reduced use of standards results from complications to replace the gas cylinders abroad (especially during the covid period), as well as to store them onboard. It is recommended to measure a complete set of standards every 3 hours. During the first week, to test the system, a complete set of standards was measured every hour. As the system behaved well and the drift of the LICOR was acceptable (less than 0.4 ppm over 6 hours), the measurement of standards was increased to every 6 hours, then every 12 hours to save the reference gases. Although not ideal, this is still more frequent than the once-a-day rate on the racing sailboats (Landschützer et al., 2023).

It is quite challenging to install such a system on a schooner, but it also presents numerous advantages, one of the most important being the shallow depth of the seawater intake. *Tara*'s seawater intake is located below the hull, at 1.5 m depth. This is shallower than on many research vessels (5 m depth on average), and better represents the actual air-sea exchanges, especially in stratified regions (Ho and Schanze, 2020). The system also has the advantage to be able to work in turbid environment. The equilibrator was cleaned regularly to avoid the buildup of mud, and the system therefore recorded data during the whole time spent in the Amazon River.

2.3. Using atmospheric CO_2 to validate the span value

It is customary to measure in the laboratory the value of each non-zero standard after the cruise as its value can differ from the value reported by the constructor. Unfortunately, this was not possible because after this long cruise (and some gas leakage in rough seas) the tank was empty. The value requested for the non-zero standard was 500 ppm, with a reported 507.9 ppm value by the supplier (Airgas), with an uncertainty of 2 %. The value measured in the laboratory before the cruise was 530 ppm. However, we found that choosing this value of 530 ppm results in unrealistically high atmospheric (close to 440 ppm) and oceanic (>450 ppm) xCO_2 measurements (blue in Fig. 3). Furthermore, it is outside of the uncertainty range reported by the manufacturer.

https://doi.org/10.5194/essd-2024-452
Preprint. Discussion started: 28 October 2024

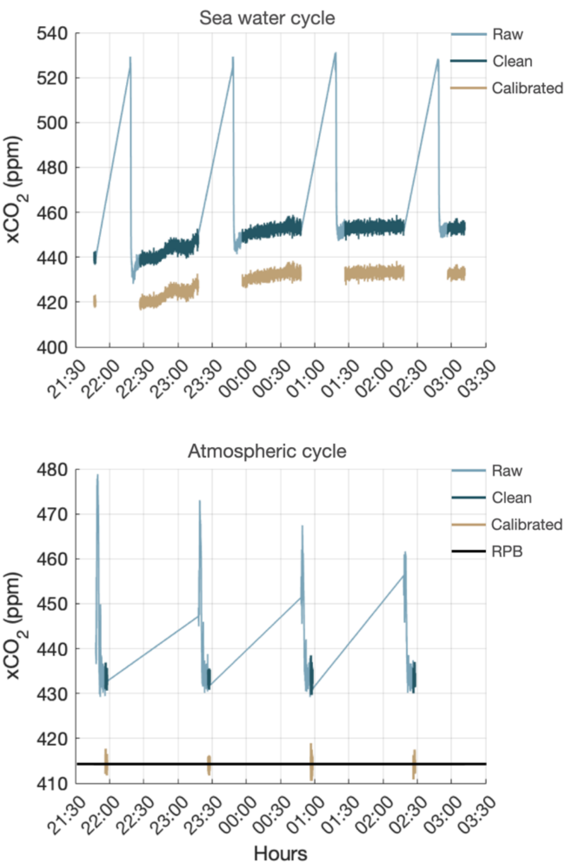

Figure 3: Time-series of *Tara* xCO_2 extracted near Barbados (night of 18-19 August 2021) for the seawater cycle (top) and atmospheric cycle (bottom). The raw data are shown in light blue, the data cleaned for valve change pollution in dark blue and the clean and calibrated data in brown. For the atmospheric cycle, the value measured at Ragged Point, Barbados (RPB) on 15 August 2021 (414.15 ppm) is shown in black.

To address this calibration issue, we take advantage of the atmospheric xCO_2 measured on board. A few days after departure, during the night from 19 to 20 August 2021, *Tara* sailed in close vicinity to the Island of Barbados, where recurrent accurate measurements of atmospheric xCO_2 are taken at Ragged Point, Barbados (RPB). The xCO_2 measured by *Tara* calibrated using the value of 530 ppm for the span was very stable over 4 hours at 437.09 ppm. The atmospheric xCO_2 measured at RPB on 15 August 2021 (closest measure to *Tara*'s passage) was 414.245 ppm. In order for the *Tara* xCO_2 data near Barbados to match the ones at RPB, the span value should be 502.3 ppm, which is within the uncertainty range provided by Airgas. This span value was then used to calibrate the entire dataset (yellow in Fig. 3). This method assumes that the atmospheric CO_2 near Barbados is representative of the value on *Tara*. During the time *Tara* was near the island, winds were moderate and blowing from the sea (not shown), so the atmospheric xCO_2 at RPB is not expected to vary much from day to day (~ 0.5 ppm). In the worst case, an error of 1 ppm in the calibration value would lead to a ± 0.84 ppm averaged difference over the dataset. *Tara*

https://doi.org/10.5194/essd-2024-452
Preprint. Discussion started: 28 October 2024

crossed highly variable regions during its voyage, supporting our confidence that the uncertainty on the dataset due to this span value is not significantly impacting the results.

2.3. Validation of the dataset

Samples of TA and DIC were taken at each station. Out of a total of 78 samples, 17 are from the surface (Metzl et al., 2024). Their salinity ranges on a salinity scale from 0 inside the Amazon River to 37.3 in the North Brazil Current. The fCO_2 is computed from the near-surface ocean DIC and TA using the CO2SYS software to compare with the continuous fCO_2 measurements (Fig. 4). The dissociation constants were taken as the one of Mehrbach refitted by Dickson and Millero (Dickson and Millero, 1987; Mehrbach et al., 1973) and nutrients were neglected. The dissociation constants used are the same as those in Lefevre et al. (2010) to ensure consistency for comparison in Section 4. However, we also tested several other sets of constants for additional analysis, detailed below. It is worth noting that DIC and TA is not the most accurate pair to determine the fCO_2, and it can lead to a probable error of 5.7 µatm (Millero et al., 1995).

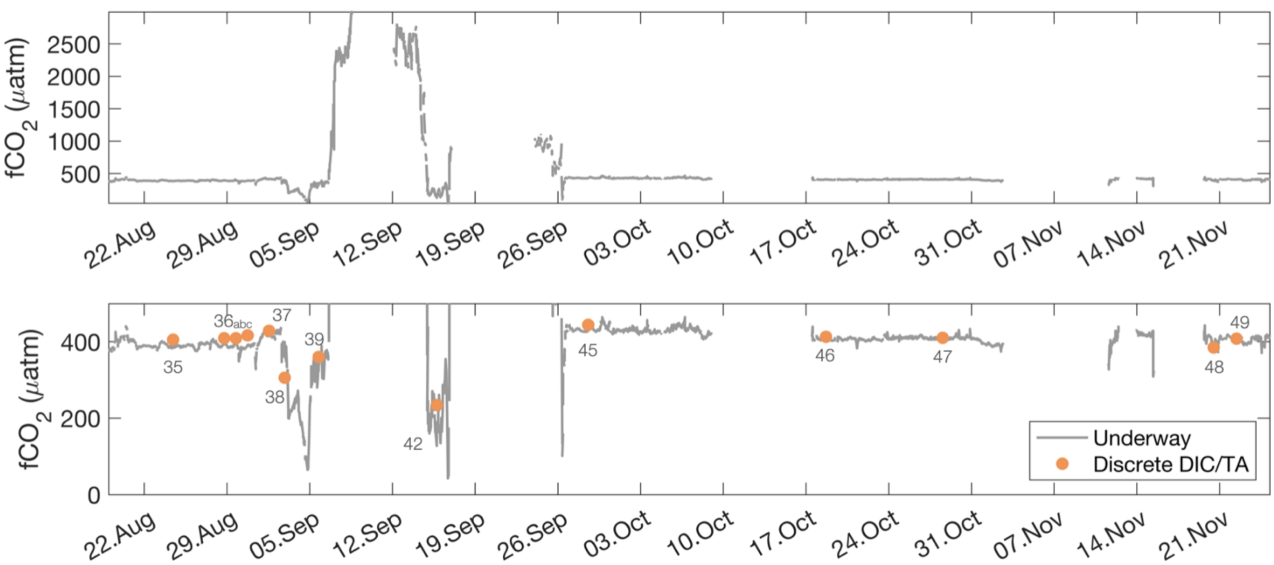

Figure 4: Time-series of the surface fCO_2 from 18/08/2021 to 25/11/2021. The lower panel focuses on a smaller range of fCO_2 values, and the dots indicate the fCO_2 inferred from the DIC/TA water samples for stations 35 to 49.

Considering the compromise on accuracy that had to be made to be able to sample on the schooner, the continuous fCO_2 compares very well to the one computed from the samples, especially after 26 September. Before that, the DIC/TA samples from the rosette during CTD casts were often taken in the presence of salinity-stratification near the surface in the ARP. The depth actually sampled for these samples is likely to be a bit deeper (couple meters) than the depth of the in-line TSG (sampling

https://doi.org/10.5194/essd-2024-452
Preprint. Discussion started: 28 October 2024

depth at 1.5 m), which could explain why the fCO_2 measured underway is lower than the one inferred from DIC/TA in the ARP. Over the whole time-series no constant bias is identified, and the mean difference after 26 September is of 2.02 µatm (standard deviation of the difference (STD_{diff}) =7.4 µatm), and drops to 0.97 µatm (STD_{diff} = 0.5 µatm) after 10 October. These results vary but stay in the same order of magnitude when changing the dissociation constants. Using constants from Lueker et al., (2000) leads to similar results (mean difference of 1.2 µatm), the largest differences are obtained using the constants from Waters et al., (2014), that are designed for a large salinity range (0-50). It improves the comparison for low salinities (before September 26) but gives slightly larger differences for high salinities (mean difference after 26 September of 0.5 µatm and 3.4 µatm after 10 October). Overall, the mean difference remains around 2 µatm, providing an estimate of the dataset's uncertainty.
As no other dataset can be used to cross-quality check the data, the good agreement between fCO_2 estimated from the samples and the continuous fCO_2 measurements is quite important, and the mean differences are in the range of uncertainties related to inferring fCO_2 from the DIC and TA measurements.

2.5. Reported data

Following the recommendations of Pierrot et al. (2009) and of SOCAT, the dataset provides for each location and time step the measured data: molar fraction of CO_2 in the equilibrator ($xCO2_{eq}$), sea surface salinity (SSS), temperatures (SST and T_{eq}), and pressure (P_{atm}), the calculated variables (pCO_{2sw}, fCO_{2sw}), and ancillary data (wind speed at 10 m). The wind speed was measured by a Gill anemometer at the top of the mast (27 m), and then adjusted to 10 m using a logarithmic relationship (Tennekes, 1973). The atmospheric fCO_2 is not included as the atmospheric xCO_2 was used as a standard and for validation of the dataset. The dataset will be submitted to the 2025 SOCAT version, with a flag C, as only one non-zero reference gas is used to calibrate the measured xCO_2. In the meantime, the data are available in the following public repository: https://zenodo.org/records/13790065 (Olivier et al., 2024a).

https://doi.org/10.5194/essd-2024-452
Preprint. Discussion started: 28 October 2024

3 Overview of the data

3.1. From the Caribbean to Uruguay

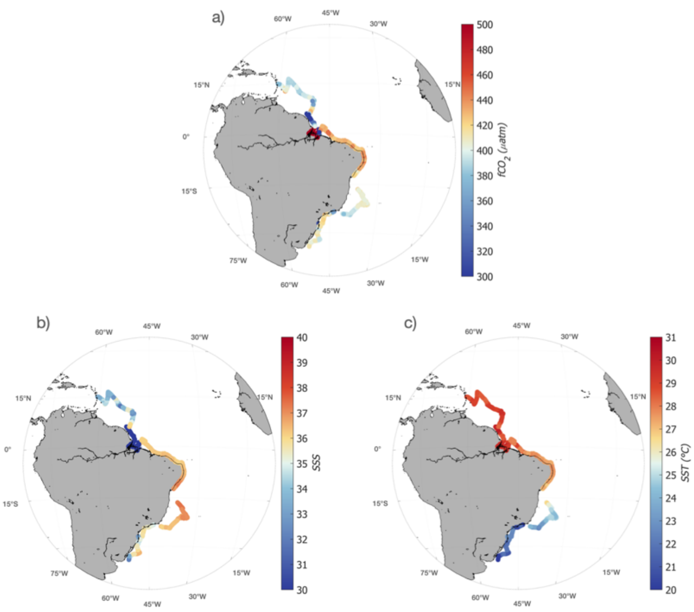

Figure 5: Along track a) CO_2 fugacity (complete range of values shown in Figure 4), b) sea surface salinity and c) sea surface temperature.

After leaving Martinique Island on 18 August 2021, *Tara* samples the Northwestern tropical Atlantic. Surface waters exhibit strong spatial variability, with salinities and temperatures changing from 31.5 to 35.5 and from 27.5 °C to 30.5°C. It reflects on the variability of the surface fCO_2, that ranges from 370 to 420 µatm (Fig. 5 and 6).

The schooner then crosses the saline (36) water of the NBC retroflection, before sampling the water of the recent ARP. Around this period of time, the ARP is located almost entirely on the shelf as salinities lower than 30 are observed at depths shallower than 100 m (Fig. 6). The ARP water is drastically different from the one of the NBC retroflection, and the two water masses are separated by strong horizontal fronts. On 3 September 2021 *Tara* crosses a front of 14.2 in salinity between 00h30 and 5h00. This first strong front is followed by several others, on 4 September between 00h and 20h (loss of 14 salinity unit), between 4 September 20h and 5 September 9h (increase of 17 salinity unit), and finally on the 6 September between 10h and 23h the salinity drops from 24.2 to 0 as the schooner reached the Amazon River. These sharp salinity fronts are associated with variations of temperature (variability of 2-3°C) and mainly fCO_2. In the ARP, the fCO_2 variations follow the ones in salinity. The fCO_2 of the ARP is extremely low, as for a salinity of 11 on 4 September a fCO_2 of 65 µatm is observed (Fig. 6). The salinity and fCO_2 increase on 5 September are associated with a decrease of SST, which could suggest an event of vertical mixing or local upwelling. This event generated fCO_2 fluctuations, and then as the schooner approaches the river and the

https://doi.org/10.5194/essd-2024-452
Preprint. Discussion started: 28 October 2024

salinity decreases, the conditions are switching from maritime to riverine and fCO_2 rapidly increases. In the Amazon River, fCO_2 is very high, reaching 3000 µatm in Macapá.

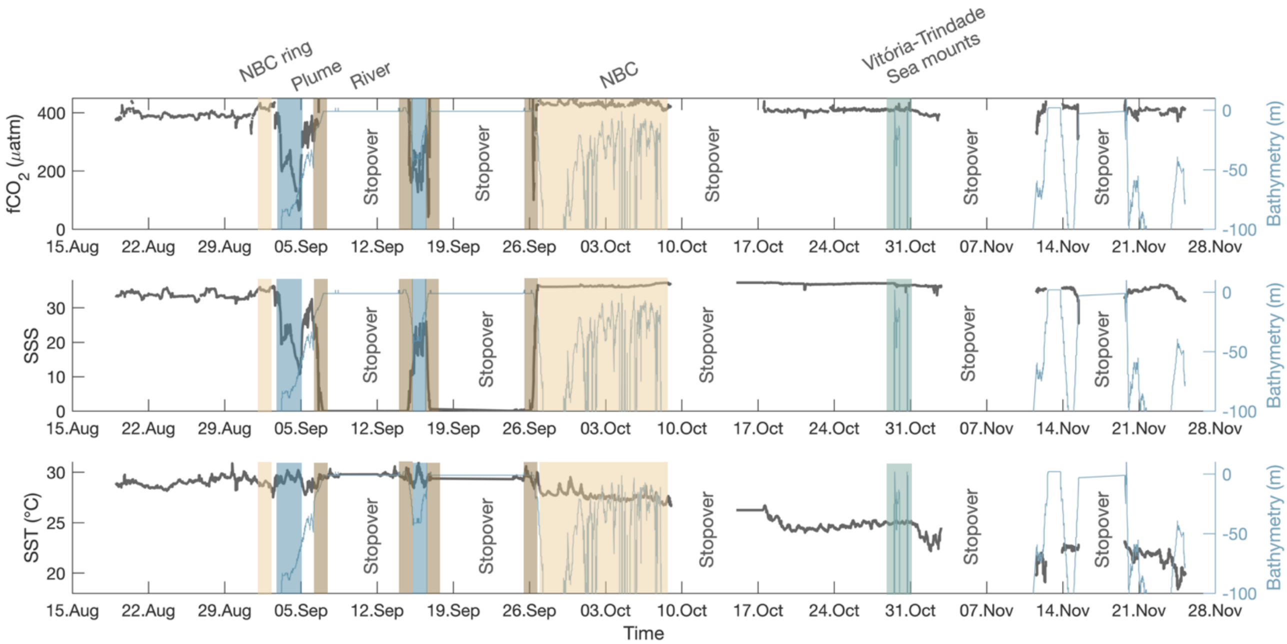

Figure 6: Time-series of fCO_2, sea surface salinity and sea surface temperature. The light blue line on each panel represents the along track ETOPO2v2 bathymetry. The shaded patches show areas of interest identified on Fig.1. NBC: North Brazil Current.

On 12 September, the schooner leaves the Amazon River and samples the Amazon and Pará Rivers plume before entering the Pará River to join Belém. The lowest fCO_2 of the time series is observed in the Amazon/ Pará River plume, with a fCO_2 of 42.8 µatm offshore of the Pará River. After the stopover in Belém, the ship samples the waters of the NBC. They stand out by their high salinity (around 37) and high fCO_2 (~ 420 µatm), and strongly contrast with the river plume waters. The temperature is decreasing and shows a variability on the order of one degree Celsius. From 9 October to 18 October the ship stops in Salvador da Bahia, and then sails to Rio de Janeiro, with a particular focus on the Vitória-Trindade Seamounts, a biodiversity hotspot (Pinheiro et al., 2015) amidst the South Atlantic Subtropical Gyre, one of the most oligotrophic zones of the global ocean (Morel et al., 2010). The temperature is significantly colder (24°C after Salvador compared to 26/27°C before), and its variability is closely associated with the one of fCO_2 (the decrease in temperature is associated with a decrease in fCO_2 close to the rate of 4.23 %/°C given by Takahashi et al., 1993). It indicates a switch from a fCO_2 variability dominated by salinity and primary production to a fCO_2 variability dominated by a temperature solubility effect. Around the Vitória-Trindade Seamounts (28 October to 1 November) we observe a strong variability of surface salinity and CO_2, correlated to the shallower bathymetry, which could be driven by upwelling turbulent mixing (Mashayek et al., 2024).

https://doi.org/10.5194/essd-2024-452
Preprint. Discussion started: 28 October 2024

The ship calls in Rio from 2 November to 11 November and then sails to Itajaí with a call in Santos. This part of the journey is very coastal, with bottom depth almost always above 100 m. It shows strong fCO_2 variability, with low values associated to the low salinities close to Santos. After 19 November, the temperature decreases as the ship sails southward and reaches a minimum of 18.4 °C, associated to a small drop in fCO_2. Salinity also decreases to 31 as bottom depth gets shallower than 50 m, possibly an early signal from the Rio de la Plata plume or/and a signal from the lagoa dos Patos.

3.2 The Amazon river-ocean continuum

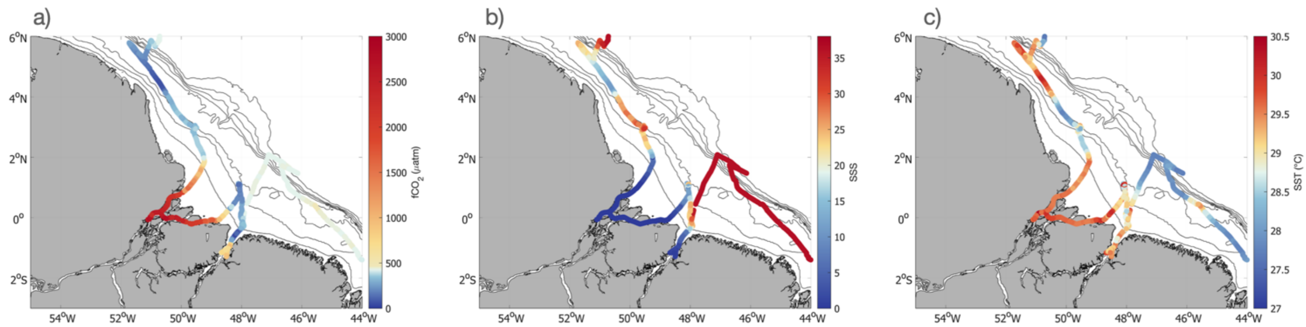

Figure 7: Along track fCO_2 (a), sea surface salinity (b) and sea surface temperature (c) in the Amazon region. Bathymetry contours are represented in black, from 10 m to 2000 m.

The largest variations of fCO_2 are observed in the AROC. The strongest gradient, reaching 3000 µatm, is observed at the transition between the maritime and riverine waters. The signature of the ARP in itself is important, with a variation of fCO_2 of up to 340 µatm (Fig. 6). In the center of the plume, the minimum observed fCO_2 is of 65 µatm, whereas outside of the plume, in the NBC, the fCO_2 is around 420 µatm. Then, on the Amazon shelf, fCO_2 progressively gets stronger as *Tara* went southward towards the Amazon, with the change in regime intensifying around the 30 m bathymetry line, when the ARP switches from a sink to a very strong source (fCO_2 > 2000 µatm, Fig. 7). The AROC is sampled twice, and so is the Pará river-ocean continuum (Fig. 6, 7).

Table 1: Coordinates of each region defined on Figures 8 and 9. On Figure 8, regions 'Open Ocean to Belém' and 'Belém to open ocean' are merged.

REGION	COORDINATES START	COORDINATES END
Open ocean to Macapá	60.8°W/15°N	51.1°W/0
Macapá to open Ocean	50.3°W/0	48°W/1.1°N
Open ocean to Belém	48°W/1.1°N	48.5°W/1.2°S
Belém to open ocean	48.5°W/1.2°S	45.8°W/0.6°N

https://doi.org/10.5194/essd-2024-452
Preprint. Discussion started: 28 October 2024

For the four crossings of the river-ocean continuum (two in the Amazon River, two in the Pará River, Table 1), different fCO_2/SSS relationships (Fig. 8) and different relationships to bathymetry (Fig. 9) are observed. From the NBC to the core of the ARP (6°N to 4°N, Fig. 8a, b), the fCO_2/SSS measurements follow well the relationship reported in Lefèvre et al., (2010, then NL). However, when salinity and fCO_2 increase locally from 4°N to 2°N, they move away from the NL linear relationship. This is even more pronounced closer to the Amazon River, where the salinity decreases (from 25 to 0) and bottom depth is shallower than 20 m (Fig. 9). After a slow decrease for salinity ranging from 25 to 12, fCO_2 sharply increases in a non-linear fashion as the bathymetry gets shallower than 20 m (salinity ranging from 12 to 5). For depth shallower than 10 m and salinities below 5, the fCO_2 is already greater than 1000 µatm and shows the largest variability (on the order of 500 µatm) before the ship enters the pure riverine waters (0 salinity, depth of ~ 2 m, Fig. 8b, 9b).

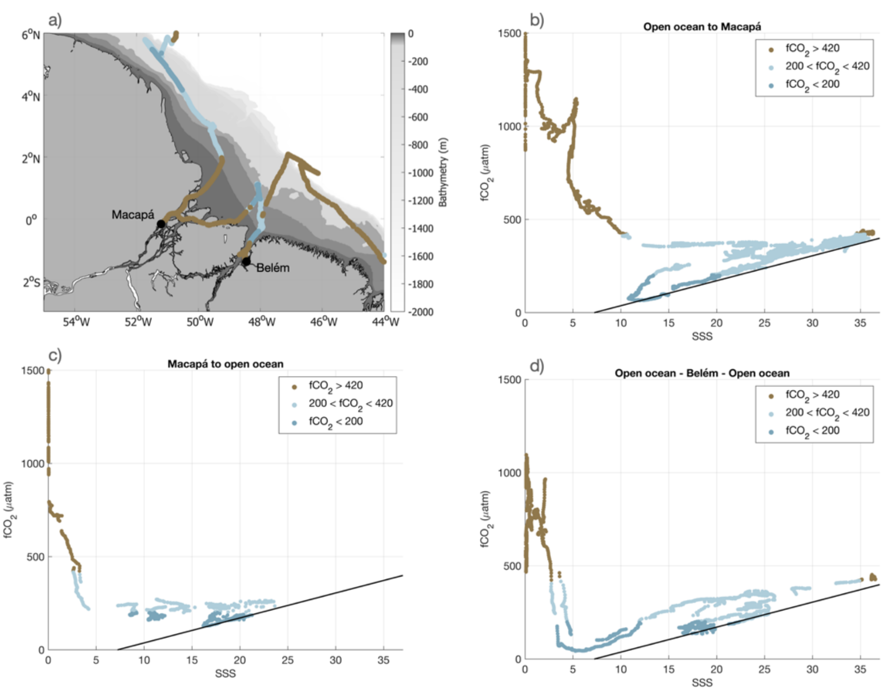

Figure 8: a) Map of the Amazon region, with bathymetry contours. Each region is defined in table 1. The track is colored based on the fCO_2 values to highlight three regimes (fCO_2 >= 420 µatm (brown), 200µatm < fCO_2 < 420µatm (light blue) and fCO_2 <= 200 µatm (dark blue)). fCO_2-SSS diagram for the entrance in the Amazon River (b) for the exit of the Amazon River (c) and for the sampling of the Pará River (d). The black line on b) c) d) is the fCO_2/SSS relationship from Lefèvre et al., (2010).

The schooner leaves the Amazon River through a different branch than on entry (Fig. 8a). The decrease in fCO_2 from 1000 µatm to 300 µatm is more linear with respect to salinity, and the source-sink transition occurs at a lower salinity than on entry (3 instead of 12, Fig. 8c). The points in the 5 to 25 salinity range show great variability, and only those with the lowest

https://doi.org/10.5194/essd-2024-452
Preprint. Discussion started: 28 October 2024

fCO_2 and salinities between 15 and 20 follow the NL relationship. The variation of salinity with bathymetry is not the same as in the way in, where the salinity stays lower than 15 for depths between 20 and 40 m.

The variation of fCO_2 along the way in the Pará River is also different from the way out, but with less variability than for the Amazon River (Fig. 8d). The sink-source transition occurs at salinities of 2.7 and 3.7 respectively and for very shallow depth (< 5 m, Fig. 9a). The minimum fCO_2 reached before the Pará River is 42.7 µatm for a salinity of 5, whereas on the way out it is 101.6 µatm for a salinity of 7. This is likely due to the Pará River plume being advected northwestward along the shelf and mixing with the ARP on its northern side. On the southern side, it mixes with the carbon-rich waters of the NBC.

The transition from a source to a sink thus presents large variability. It doesn't happen at a consistent salinity or bottom depth, highlighting the role of other parameters driving the fCO_2 variability in the region.

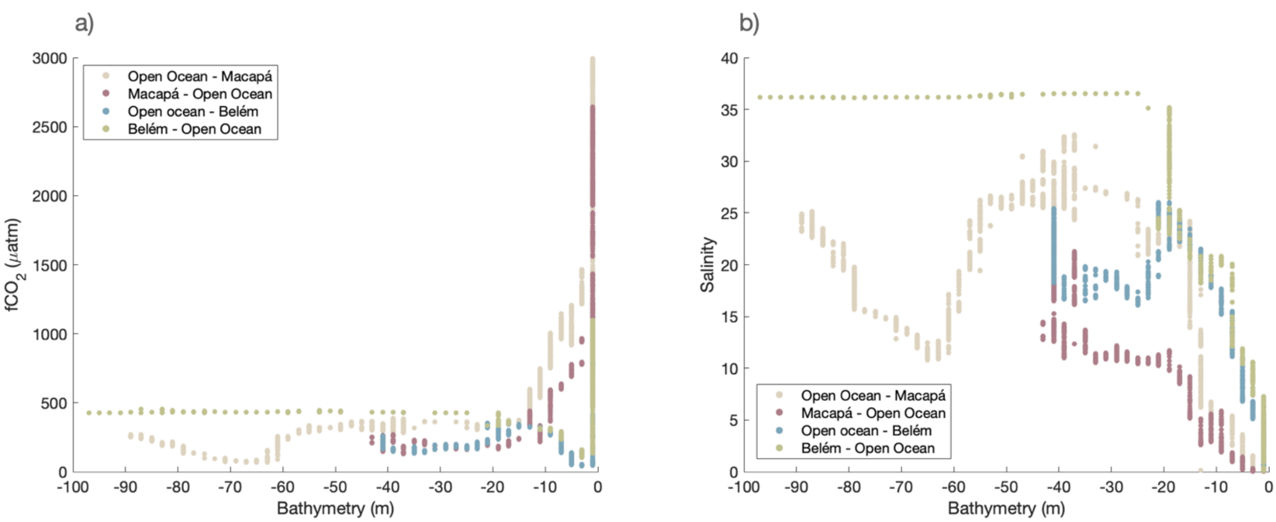

Figure 9: a) fCO_2-bathymetry and b) SSS-bathymetry of the different river-ocean continuum crossings for depths shallower than 95 m. The bathymetry is ETOPO2v2 colocalized along the ship track.

4 Discussion

4.1 Main drivers of fCO_2 variability

4.1.1 Salinity

In the tropical band (15°N-15°S) of the western Atlantic, the fCO_2 variability in the data follows well the strong surface salinity variability (Fig. 6). There are two reasons for that. First, in this region, the surface temperature is very warm (SST>27°C), with relatively small variability (the STD of the SST in the dataset is of 0.8°C). The solubility effect associated to an increase in temperature of 0.8 °C would be an increase of the fCO_2 by 13.6 µatm (Takahashi et al. 1993, 4.23%/°C). While this is non-negligeable, it is small compared to the observed STD of 109 µatm observed in the *Tara* dataset between 15°N and 15°S (excluding waters with SSS<=1).

Second, the Amazon River flows into the tropical Atlantic and forms huge salinity gradients (STD of the SSS in the *Tara* dataset between 15°N and 15°S is of 7.5 (for SSS>1)). These gradients indicate the river's influence on the open ocean, and thus also the changes in biogeochemical and biological properties. At first order, the gradient in salinity is indicative the gradient in alkalinity and DIC (linked to biological activity) associated to the river plume and therefore fCO_2. This explains the robustness of empirical linear relationships between salinity and fCO_2 in the ARP, such as the one of Lefèvre et al., (2010), presented in part 3.2. The good agreement for a reasonable salinity range of this new dataset with the pre-existing relationship a further validation of the quality of the data.

4.1.2 Temperature

South of 15°S, the situation is different, with larger temperature changes. As the schooner sails poleward, the temperature decreases with no more influence of the Amazon River system. At first order, the fCO_2 variations follow the one expected from the solubility effect. The SST decreases of 8°C, and the change in fCO_2, with a maximum of 442.8 µatm and a minimum of 309.2 µatm, is coherent with a drop of 8°C in temperature (expected drop in fCO_2 of 136 µatm following a 4.23 %/°C effect; Takahashi et al., 1993).

Nevertheless, while the large-scale variability of the fCO_2 reflects the latitudinal temperature gradient, at smaller scales the variability of salinity is also important and different water masses are sampled. Notably, south of Rio de Janeiro, the schooner sails on the shelf, with a bathymetry often shallower than 100 m. Other river discharges reach the south Atlantic, such as the one of the Rio de la Plata. These waters spread on the shelf and generate variability in salinity, suspended sediments and biological activity.

4.2 The sink-source transition in the river-ocean continuum

The multiple crossings of the river-ocean continuum show a great fCO_2 variability in the Amazon River/ Pará River estuaries and resulting plumes on the Amazon shelf. As a continuous feature, this environment can extend over 500 km along-shelf and 200 km across-shelf (Curtin and Legeckis, 1986). Within this region, the transports of fresh water, sediment, nutrients and biomass are determined by energetic processes occurring on semidiurnal, several-day, several-week and seasonal time scales (Curtin, 1986; Geyer et al., 1991).

https://doi.org/10.5194/essd-2024-452
Preprint. Discussion started: 28 October 2024

In the regions close to the river estuary, the fCO_2 changes are no longer primarily associated with the changes in salinity anymore. As salinity decreases, the switch from a decreasing fCO_2 (representative of the plume) to increasing fCO_2 (representative of the river) does not happen at the same salinity for each crossing. Moreover, the linear relationship between salinity and fCO_2 does not hold close to the river. It is thus likely that the salinity gradient no longer mirrors the gradient in DIC or in TA. The strong sediment load of the Amazon River prevents the light penetration in the water column and the development of photosynthetic organisms (DeMaster et al., 1986). The source to sink transition is mainly driven by the switch from a respiration dominated system to a photosynthetic one. Several factors impact the suspension of sediments in the water column and the development of phytoplankton, such as the bathymetry, winds and the tides. Indeed, tides and tidal currents are one of the dominant factors of the variability of the Amazon estuary with tidal currents ranging from 0.5 to 2.0 m s^{-1} (Geyer et al., 1991).

The relationship between suspended sediments and bathymetry allowed the identification of 4 zones of interactions by Curtin & Legeckis (1986). They match well with the fCO_2 measurements. For the Amazon River, the zone of highest suspended sediments concentration (SSC) is located between the isobaths 4 m and 11 m, matching the strong increase of the fCO_2 observed for the two crossings of the AROC. The zone of lowest SSC is between the isobaths 10 m and 20 m, associated to a diatom bloom in 1983 (Curtin and Legeckis, 1986; DeMaster et al., 1986). It is also the region where we observe the transition from a source to a sink of CO_2 (Fig. 9). For the Pará River, this region extends directly to the mouth, for depth shallower than 5 m. It also matches the observations, and the differences between the two rivers. Indeed, while for the Amazon River, the transition from a sink to a source happens between 10 and 20-m depth, it happens at much shallower depths for the Pará River (below 10 m). Their "River Zone", for depth below 5 m, indeed corresponds to a salinity of 0. Nevertheless, we observe significant variability of fCO_2 even if the salinity does not change anymore. This region was not investigated by these studies that focused further offshore of the mouth. Therefore, combining the fCO_2 dataset and the numerous optical measurements also conducted underway onboard the *Tara* Mission Microbiome could lead to a better understanding of the AROC system. Moreover, linking this continuous dataset to the discrete imaging and genetic samples from Mission Microbiome's stations, conducted in the different zones of the system, will also bring light on the biological communities responsible for the strong CO_2 source or sink observed.

4.3 Limitations of the dataset

Onboard *Tara*, there is rarely a trained scientist to take care of an equilibrator fCO_2 system. The system therefore has to run almost autonomously, and is monitored from land when someone trained is not onboard. Limited space meant that only two standards were used, and they were stored outside on the foredeck. The deck is subject to spray, waves and wave-related impacts. This increases the strain on the system, and the possibility of failure, in particularly during bad weather. The fCO_2 system operations were finally terminated due to several leakages that happened during the strong sea state encountered in the Southern Ocean. For this mission, *Tara* sampled mainly coastal environments, where CO_2 is highly variable and little known. There are very little previously acquired data in the region that can be used for comparison. And even where there are other data, the variability in the coastal ocean is such that it might not be comparable. Some surface samples of DIC and TA were collected by scientists on board, which were essential to validate the fCO_2 measured. The mean difference of 2 µatm and STD_{diff} of 7.4 µatm (going down to 0.5 µatm in the less variable environment) give an estimate of the uncertainty that support the validity of the dataset. It is nevertheless necessary to note that the relationship to compute fCO_2 from DIC and TA also has an uncertainty of 5.4 µatm, and it would be more accurate to compare with fCO_2 measurements if they would exist. This shows the limitation of autonomous fCO_2 systems that cannot be checked regularly, and especially the ones on small boats that are more fragile due to the rougher conditions than on a large research or container ship.

5 Conclusion

For the first time, a schooner equipped with a fCO_2 equilibrator system measured fCO_2 along the eastern coasts of South America. This high temporal resolution dataset includes fCO_2 measurements every minute over 14,000 km of sailing. From the Caribbean to Argentina, this 4-month dataset of 65,000 measurements (from August to December 2021) shows large fCO_2 variability with a standard deviation of 480 µatm. In particular, it sampled the Amazon River plume, the Amazon and Pará River estuaries, the North Brazil Current, the Brazil Current, the Vitória-Trindade Sea mounts (local hotspot of biodiversity), and the shelves of southern Brazil.

In August-September 2021, the Amazon-Pará plume is highly undersaturated with CO_2, in line with the many regional studies on the Amazon River plume (Ibánhez et al., 2015; Körtzinger, 2003; Lefévre et al., 2010; Mu et al., 2021). This dataset provides data closer to the river than in some of these earlier studies, sampling the heart of the plume. Further from the mouth, fCO2 reaches extreme low values, between 40 and 60 µatm, which had never been observed before. It is possible to measure such low values because for the first time a ship equipped with a fCO_2 system is sampling the river-ocean continuum, and pumping water at a very shallow depth. When salinity continues to drop ($S<8$), a sink-source transition occurs, and fCO_2 rises rapidly. The influence of the river becomes dominant, and fCO_2 reaches 3000 µatm in the river. The river-ocean continuum has been crossed four times, and each time showed different properties. This system is highly dynamic and needs to be studied further in depth to infer the global role of the Amazon system in the global carbon budget.

Equipping a sailboat with a fCO_2 equilibrator system is a challenge, but one that has been met by the schooner *Tara*. The dataset is very valuable for global and regional studies, filling part of the data gap in the coastal regions of the South Atlantic Ocean. It is particularly helpful for fCO2 mapping products, which assimilate all data collected to produce global monthly and climatological fCO2 maps from neural network reconstruction (Chau et al., 2024; Denvil-Sommer et al., 2019; Landschützer et al., 2016, 2020; Laruelle et al., 2017). It is also useful for process studies, such as the river-ocean continuum (Sawakuchi et

https://doi.org/10.5194/essd-2024-452
Preprint. Discussion started: 28 October 2024

al., 2017), offshore ARP (Olivier et al., 2024b), the Guanabara Bay (Cotovicz Jr et al., 2015), and the coastal currents of the South American coast. The difficulty in validating the dataset shows just how little is known about coastal regions and how dynamic they are. Despite sampling most of the American coastline along the South Atlantic Ocean, it represents only a small fraction of the world's coastlines. Collecting more fCO_2 data in under-sampled regions, such as the southern hemisphere oceans, the Southern Ocean, coastal regions and estuaries, is very important to improve our knowledge of the global carbon cycle (Roobaert et al., 2019).

Data availability

The dataset is available in the following public repository: https://doi.org/10.5281/zenodo.13790065 (Olivier et al., 2024a), with the DOI 10.5281/zenodo.13790065. It is also submitted to the SOCAT version 2025.

Author contribution

LO, JB and GR conceptualized the project. LO, TL, NH and AC collected the data and LO and CH curated the data. CH and DV designed and provided the instrument to collect the dataset. SP managed and coordinated the project on land and on board for the mission. LO prepared the manuscript with contributions from all co-authors.

Competing interests

The authors declare that they have no conflict of interest.

Acknowledgements

We wish to thank the Tara Ocean Foundation, the SV *Tara* crew and all those who participate in Mission Microbiomes AtlantECO and adopt its Data Sharing & Publication Best Practices(https://zenodo.org/communities/mission-microbiomes-atlanteco/). In particular, we would like to thank chief engineer Léo Boulon for all his help with the installation of the system as well as Martin Hertau, Nicolas Bin and Samuel Audrain for the maintenance. Clémentine Moulin and Aliénor Bourdais, thank you for the help with the logistics, the shipping and the coordination. We warmly thank the SNAPOCO_2 and Jonathan Fin for the precious accurate analysis of the DIC/TA samples. We are keen to thank the commitment of the following institutions for their financial and scientific support that made Mission Microbiomes AtlantECO possible: Stazione Zoologica Anton Dohrn, European Bioinformatics Institute (EMBL-EBI), Centre national de la recherche scientifique (CNRS), Centre National de Séquençage (CNS, Genoscope), agnès b., BIC, Capgemini Engineering, Fondation Groupe EDF, Compagnie Nationale du Rhône, L'Oréal, Biotherm, Région Bretagne, Lorient Agglomération, Billerudkorsnas, Havas Paris, Fondation Rothschild, Office Français de la Biodiversité, AmerisourceBergen, Philgood Foundation, UNESCO-IOC, Etienne Bourgois.

Financial support

https://doi.org/10.5194/essd-2024-452
Preprint. Discussion started: 28 October 2024

This publication has received funding from the European Union's Horizon 2020 research and innovation programme under grant agreement No 862923 (project AtlantECO). This output reflects only the author's view and the European Union cannot be held responsible for any use that may be made of the information contained therein. This work was supported by the Initiative and Networking Fund of the Helmholtz Association (Grant Number: VH-NG-19-33). P.C.J. was supported by Fundação de Amparo à Pesquisa do Estado de São Paulo (FAPESP; PhD grant no. 2017/26786-1) and by FAI/UFSCar (ProEx no. 3213/2020-83) through the European Union—H2020 project AtlantECO (award no. 862923).

References

Araujo, M., Noriega, C., Hounsou-gbo, G. A., Veleda, D., Araujo, J., Bruto, L., Feitosa, F., Flores-Montes, M., Lefèvre, N., Melo, P., Otsuka, A., Travassos, K., Schwamborn, R., and Neumann-Leitão, S.: A Synoptic Assessment of the Amazon River-Ocean Continuum during Boreal Autumn: From Physics to Plankton Communities and Carbon Flux, Front. Microbiol., 8, 2017.

Bakker, D. C. E., Pfeil, B., Landa, C. S., Metzl, N., O'Brien, K. M., Olsen, A., Smith, K., Cosca, C., Harasawa, S., Jones, S. D., Nakaoka, S., Nojiri, Y., Schuster, U., Steinhoff, T., Sweeney, C., Takahashi, T., Tilbrook, B., Wada, C., Wanninkhof, R., Alin, S. R., Balestrini, C. F., Barbero, L., Bates, N. R., Bianchi, A. A., Bonou, F., Boutin, J., Bozec, Y., Burger, E. F., Cai, W.-J., Castle, R. D., Chen, L., Chierici, M., Currie, K., Evans, W., Featherstone, C., Feely, R. A., Fransson, A., Goyet, C., Greenwood, N., Gregor, L., Hankin, S., Hardman-Mountford, N. J., Harlay, J., Hauck, J., Hoppema, M., Humphreys, M. P., Hunt, C. W., Huss, B., Ibánhez, J. S. P., Johannessen, T., Keeling, R., Kitidis, V., Körtzinger, A., Kozyr, A., Krasakopoulou, E., Kuwata, A., Landschützer, P., Lauvset, S. K., Lefèvre, N., Lo Monaco, C., Manke, A., Mathis, J. T., Merlivat, L., Millero, F. J., Monteiro, P. M. S., Munro, D. R., Murata, A., Newberger, T., Omar, A. M., Ono, T., Paterson, K., Pearce, D., Pierrot, D., Robbins, L. L., Saito, S., Salisbury, J., Schlitzer, R., Schneider, B., Schweitzer, R., Sieger, R., Skjelvan, I., Sullivan, K. F., Sutherland, S. C., Sutton, A. J., Tadokoro, K., Telszewski, M., Tuma, M., van Heuven, S. M. A. C., Vandemark, D., Ward, B., Watson, A. J., and Xu, S.: A multi-decade record of high-quality $f\mathrm{CO_2}$ data in version 3 of the Surface Ocean CO_2 Atlas (SOCAT), Earth Syst. Sci. Data, 8, 383–413, https://doi.org/10.5194/essd-8-383-2016, 2016.

Bauer, J. E., Cai, W.-J., Raymond, P. A., Bianchi, T. S., Hopkinson, C. S., and Regnier, P. A. G.: The changing carbon cycle of the coastal ocean, Nature, 504, 61–70, https://doi.org/10.1038/nature12857, 2013.

Borges, A. V.: Do we have enough pieces of the jigsaw to integrate CO2 fluxes in the coastal ocean?, Estuaries, 28, 3–27, https://doi.org/10.1007/BF02732750, 2005.

Bork, P., Bowler, C., de Vargas, C., Gorsky, G., Karsenti, E., and Wincker, P.: Tara Oceans studies plankton at planetary scale, Science, 348, 873–873, https://doi.org/10.1126/science.aac5605, 2015.

Cai, W.-J., Dai, M., and Wang, Y.: Air-sea exchange of carbon dioxide in ocean margins: A province-based synthesis, Geophys. Res. Lett., 33, https://doi.org/10.1029/2006GL026219, 2006.

Chau, T.-T.-T., Gehlen, M., Metzl, N., and Chevallier, F.: CMEMS-LSCE: a global, 0.25°, monthly reconstruction of the surface ocean carbonate system, Earth Syst. Sci. Data, 16, 121–160, https://doi.org/10.5194/essd-16-121-2024, 2024.

Chen, C.-T. A., Huang, T.-H., Chen, Y.-C., Bai, Y., He, X., and Kang, Y.: Air–sea exchanges of CO2 in the world's coastal seas, Biogeosciences, 10, 6509–6544, https://doi.org/10.5194/bg-10-6509-2013, 2013.

Cooley, S. R., Coles, V. J., Subramaniam, A., and Yager, P. L.: Seasonal variations in the Amazon plume-related atmospheric carbon sink: SEASONALITY OF CO_2 IN AMAZON PLUME, Glob. Biogeochem. Cycles, 21, n/a-n/a, https://doi.org/10.1029/2006GB002831, 2007.

Cotovicz Jr, L. C., Knoppers, B. A., Brandini, N., Costa Santos, S. J., and Abril, G.: A strong CO_2 sink enhanced by eutrophication in a tropical coastal embayment (Guanabara Bay, Rio de Janeiro, Brazil), Biogeosciences, 12, 6125–6146, 2015.

Curtin, T. B.: Physical observations in the plume region of the Amazon River during peak discharge—II. Water masses, Cont. Shelf Res., 6, 53–71, https://doi.org/10.1016/0278-4343(86)90053-1, 1986.

Curtin, T. B. and Legeckis, R. V.: Physical observations in the plume region of the Amazon River during peak discharge—I. Surface variability, Cont. Shelf Res., 6, 31–51, https://doi.org/10.1016/0278-4343(86)90052-X, 1986.

Dai, A. and Trenberth, K. E.: Estimates of Freshwater Discharge from Continents: Latitudinal and Seasonal Variations, J. Hydrometeorol., 3, 660–687, https://doi.org/10.1175/1525-7541(2002)003<0660:EOFDFC>2.0.CO;2, 2002.

DeMaster, D. J., Kuehl, S. A., and Nittrouer, C. A.: Effects of suspended sediments on geochemical processes near the mouth of the Amazon River: examination of biological silica uptake and the fate of particle-reactive elements, Cont. Shelf Res., 6, 107–125, https://doi.org/10.1016/0278-4343(86)90056-7, 1986.

Denvil-Sommer, A., Gehlen, M., Vrac, M., and Mejia, C.: LSCE-FFNN-v1: a two-step neural network model for the reconstruction of surface ocean *p*CO_2 over the global ocean, Geosci. Model Dev., 12, 2091–2105, https://doi.org/10.5194/gmd-12-2091-2019, 2019.

Dickson, A. G.: Guide to best practices for ocean CO2 measurements, PICES Spec. Publ., 191, 2007.

Dickson, A. G. and Millero, F. J.: A comparison of the equilibrium constants for the dissociation of carbonic acid in seawater media, Deep Sea Res. Part Oceanogr. Res. Pap., 34, 1733–1743, https://doi.org/10.1016/0198-0149(87)90021-5, 1987.

Friedlingstein, P., O'Sullivan, M., Jones, M. W., Andrew, R. M., Bakker, D. C. E., Hauck, J., Landschützer, P., Le Quéré, C., Luijkx, I. T., Peters, G. P., Peters, W., Pongratz, J., Schwingshackl, C., Sitch, S., Canadell, J. G., Ciais, P., Jackson, R. B., Alin, S. R., Anthoni, P., Barbero, L., Bates, N. R., Becker, M., Bellouin, N., Decharme, B., Bopp, L., Brasika, I. B. M., Cadule, P., Chamberlain, M. A., Chandra, N., Chau, T.-T.-T., Chevallier, F., Chini, L. P., Cronin, M., Dou, X., Enyo, K., Evans, W., Falk, S., Feely, R. A., Feng, L., Ford, D. J., Gasser, T., Ghattas, J., Gkritzalis, T., Grassi, G., Gregor, L., Gruber, N., Gürses, Ö., Harris, I., Hefner, M., Heinke, J., Houghton, R. A., Hurtt, G. C., Iida, Y., Ilyina, T., Jacobson, A. R., Jain, A., Jarníková, T., Jersild, A., Jiang, F., Jin, Z., Joos, F., Kato, E., Keeling, R. F., Kennedy, D., Klein Goldewijk, K., Knauer, J., Korsbakken, J. I., Körtzinger, A., Lan, X., Lefèvre, N., Li, H., Liu, J., Liu, Z., Ma, L., Marland, G., Mayot, N., McGuire, P. C., McKinley, G. A., Meyer, G., Morgan, E. J., Munro, D. R., Nakaoka, S.-I., Niwa, Y., O'Brien, K. M., Olsen, A., Omar, A. M., Ono, T., Paulsen, M., Pierrot, D., Pocock, K., Poulter, B., Powis, C. M., Rehder, G., Resplandy, L., Robertson, E., Rödenbeck, C., Rosan, T. M., Schwinger, J., Séférian, R., et al.: Global Carbon Budget 2023, Earth Syst. Sci. Data, 15, 5301–5369,

https://doi.org/10.5194/essd-2024-452
Preprint. Discussion started: 28 October 2024

https://doi.org/10.5194/essd-15-5301-2023, 2023.

Geyer, W. R., Beardsley, R. C., Candela, J., Castro, B. M., Legeckis, R. V., Lentz, S. J., Limeburner, R., Miranda, L. B., and Trowbridge, J. H.: The physical oceanography of the Amazon outflow, Oceanography, 4, 8–14, 1991.

Ho, D. T. and Schanze, J. J.: Precipitation-induced reduction in surface ocean pCO2: Observations from the eastern tropical Pacific Ocean, Geophys. Res. Lett., 47, e2020GL088252, 2020.

Ibánhez, J. S. P., Diverrès, D., Araujo, M., and Lefèvre, N.: Seasonal and interannual variability of sea-air CO2 fluxes in the tropical Atlantic affected by the Amazon River plume, Glob. Biogeochem. Cycles, 29, 1640–1655, https://doi.org/10.1002/2015GB005110, 2015.

Körtzinger, A.: A significant CO2 sink in the tropical Atlantic Ocean associated with the Amazon River plume, Geophys. Res. Lett., 30, https://doi.org/10.1029/2003GL018841, 2003.

Landschützer, P., Gruber, N., and Bakker, D. C. E.: Decadal variations and trends of the global ocean carbon sink, Glob. Biogeochem. Cycles, 30, 1396–1417, https://doi.org/10.1002/2015GB005359, 2016.

Landschützer, P., Laruelle, G. G., Roobaert, A., and Regnier, P.: A uniform $p\mathrm{CO_2}$ climatology combining open and coastal oceans, Earth Syst. Sci. Data, 12, 2537–2553, https://doi.org/10.5194/essd-12-2537-2020, 2020.

Landschützer, P., Tanhua, T., Behncke, J., and Keppler, L.: Sailing through the southern seas of air–sea CO2 flux uncertainty, Philos. Trans. R. Soc. Math. Phys. Eng. Sci., 381, 20220064, https://doi.org/10.1098/rsta.2022.0064, 2023.

Laruelle, G. G., Lauerwald, R., Pfeil, B., and Regnier, P.: Regionalized global budget of the CO2 exchange at the air-water interface in continental shelf seas, Glob. Biogeochem. Cycles, 28, 1199–1214, https://doi.org/10.1002/2014GB004832, 2014.

Laruelle, G. G., Landschützer, P., Gruber, N., Tison, J.-L., Delille, B., and Regnier, P.: Global high-resolution monthly $p\mathrm{CO_2}$ climatology for the coastal ocean derived from neural network interpolation, Biogeosciences, 14, 4545–4561, https://doi.org/10.5194/bg-14-4545-2017, 2017.

Lefévre, N., Diverrés, D., and Gallois, F.: Origin of CO2 undersaturation in the western tropical Atlantic, Tellus B Chem. Phys. Meteorol., 62, 595–607, https://doi.org/10.1111/j.1600-0889.2010.00475.x, 2010.

Lefèvre, N., Flores Montes, M., Gaspar, F. L., Rocha, C., Jiang, S., De Araújo, M. C., and Ibánhez, J. S. P.: Net Heterotrophy in the Amazon Continental Shelf Changes Rapidly to a Sink of CO2 in the Outer Amazon Plume, Front. Mar. Sci., 4, 2017.

Lueker, T. J., Dickson, A. G., and Keeling, C. D.: Ocean *p*CO2 calculated from dissolved inorganic carbon, alkalinity, and equations for $K1$ and $K2$: validation based on laboratory measurements of CO2 in gas and seawater at equilibrium, Mar. Chem., 70, 105–119, https://doi.org/10.1016/S0304-4203(00)00022-0, 2000.

Mashayek, A., Gula, J., Baker, L. E., Naveira Garabato, A. C., Cimoli, L., Riley, J. J., and de Lavergne, C.: On the role of seamounts in upwelling deep-ocean waters through turbulent mixing, Proc. Natl. Acad. Sci., 121, e2322163121, 2024.

Mayorga, E., Aufdenkampe, A. K., Masiello, C. A., Krusche, A. V., Hedges, J. I., Quay, P. D., Richey, J. E., and Brown, T. A.: Young organic matter as a source of carbon dioxide outgassing from Amazonian rivers, Nature, 436, 538–541, 2005.

Mehrbach, C., Culberson, C. H., Hawley, J. E., and Pytkowicx, R. M.: Measurement of the Apparent Dissociation Constants of Carbonic Acid in Seawater at Atmospheric Pressure1, Limnol. Oceanogr., 18, 897–907,

https://doi.org/10.5194/essd-2024-452
Preprint. Discussion started: 28 October 2024

https://doi.org/10.4319/lo.1973.18.6.0897, 1973.

Metzl, N., Fin, J., Lo Monaco, C., Mignon, C., Alliouane, S., Antoine, D., Bourdin, G., Boutin, J., Bozec, Y., Conan, P., Coppola, L., Diaz, F., Douville, E., Durrieu de Madron, X., Gattuso, J.-P., Gazeau, F., Golbol, M., Lansard, B., Lefèvre, D., Lefèvre, N., Lombard, F., Louanchi, F., Merlivat, L., Olivier, L., Petrenko, A., Petton, S., Pujo-Pay, M., Rabouille, C., Reverdin, G., Ridame, C., Tribollet, A., Vellucci, V., Wagener, T., and Wimart-Rousseau, C.: A synthesis of ocean total alkalinity and dissolved inorganic carbon measurements from 1993 to 2022: the SNAPO-CO2-v1 dataset, Earth Syst. Sci. Data, 16, 89–120, https://doi.org/10.5194/essd-16-89-2024, 2024.

Morel, A., Claustre, H., and Gentili, B.: The most oligotrophic subtropical zones of the global ocean: similarities and differences in terms of chlorophyll and yellow substance, Biogeosciences, 7, 3139–3151, https://doi.org/10.5194/bg-7-3139-2010, 2010.

Mu, L., Gomes, H. do R., Burns, S. M., Goes, J. I., Coles, V. J., Rezende, C. E., Thompson, F. L., Moura, R. L., Page, B., and Yager, P. L.: Temporal Variability of Air-Sea CO2 flux in the Western Tropical North Atlantic Influenced by the Amazon River Plume, Glob. Biogeochem. Cycles, 35, e2020GB006798, https://doi.org/10.1029/2020GB006798, 2021.

Olivier, L., Boutin, J., Reverdin, G., Lefèvre, N., Landschützer, P., Speich, S., Karstensen, J., Labaste, M., Noisel, C., Ritschel, M., Steinhoff, T., and Wanninkhof, R.: Wintertime process study of the North Brazil Current rings reveals the region as a larger sink for CO_2 than expected, Biogeosciences, 19, 2969–2988, https://doi.org/10.5194/bg-19-2969-2022, 2022.

Olivier, L., Reverdin, G., Boutin, J., Hunt, C., Linkowski, T., Chase, A. P., Haentjens, N., Junger, P. C., Pesant, S., and Vandemark, D.: CO2 fugacity aboard the schooner Tara during Mission Microbiomes AtlantECO., https://doi.org/10.5281/zenodo.13790064, 2024a.

Olivier, L., Reverdin, G., Boutin, J., Laxenaire, R., Iudicone, D., Pesant, S., Calil, P. H. R., Horstmann, J., Couet, D., Erta, J. M., Huber, P., Sarmento, H., Freire, A., Koch-Larrouy, A., Vergely, J.-L., Rousselot, P., and Speich, S.: Late summer northwestward Amazon plume pathway under the action of the North Brazil Current rings, Remote Sens. Environ., 307, 114165, https://doi.org/10.1016/j.rse.2024.114165, 2024b.

Pesant, S., Not, F., Picheral, M., Kandels-Lewis, S., Le Bescot, N., Gorsky, G., Iudicone, D., Karsenti, E., Speich, S., Troublé, R., Dimier, C., and Searson, S.: Open science resources for the discovery and analysis of Tara Oceans data, Sci. Data, 2, 150023, https://doi.org/10.1038/sdata.2015.23, 2015.

Pierrot, D., Neill, C., Sullivan, K., Castle, R., Wanninkhof, R., Lüger, H., Johannessen, T., Olsen, A., Feely, R. A., and Cosca, C. E.: Recommendations for autonomous underway pCO2 measuring systems and data-reduction routines, Deep Sea Res. Part II Top. Stud. Oceanogr., 56, 512–522, https://doi.org/10.1016/j.dsr2.2008.12.005, 2009.

Pinheiro, H. T., Mazzei, E., Moura, R. L., Amado-Filho, G. M., Carvalho-Filho, A., Braga, A. C., Costa, P. A. S., Ferreira, B. P., Ferreira, C. E. L., Floeter, S. R., Francini-Filho, R. B., Gasparini, J. L., Macieira, R. M., Martins, A. S., Olavo, G., Pimentel, C. R., Rocha, L. A., Sazima, I., Simon, T., Teixeira, J. B., Xavier, L. B., and Joyeux, J.-C.: Fish Biodiversity of the Vitória-Trindade Seamount Chain, Southwestern Atlantic: An Updated Database, PLOS ONE, 10, e0118180, https://doi.org/10.1371/journal.pone.0118180, 2015.

Roobaert, A., Laruelle, G. G., Landschützer, P., Gruber, N., Chou, L., and Regnier, P.: The Spatiotemporal Dynamics of the Sources and Sinks of CO2 in the Global Coastal Ocean, Glob. Biogeochem. Cycles, 33, 1693–1714, https://doi.org/10.1029/2019GB006239, 2019.

Sawakuchi, H. O., Neu, V., Ward, N. D., Barros, M. de L. C., Valerio, A. M., Gagne-Maynard, W., Cunha, A. C., Less, D. F. S., Diniz, J. E. M., Brito, D. C., Krusche, A. V., and Richey, J. E.: Carbon Dioxide Emissions along the Lower Amazon River, Front. Mar. Sci., 4, 2017.

Subramaniam, A., Yager, P. L., Carpenter, E. J., Mahaffey, C., Björkman, K., Cooley, S., Kustka, A. B., Montoya, J. P., Sañudo-Wilhelmy, S. A., Shipe, R., and Capone, D. G.: Amazon River enhances diazotrophy and carbon sequestration in the tropical North Atlantic Ocean, Proc. Natl. Acad. Sci., 105, 10460–10465, https://doi.org/10.1073/pnas.0710279105, 2008.

Takahashi, T., Olafsson, J., Goddard, J. G., Chipman, D. W., and Sutherland, S. C.: Seasonal variation of CO2 and nutrients in the high-latitude surface oceans: A comparative study, Glob. Biogeochem. Cycles, 7, 843–878, https://doi.org/10.1029/93GB02263, 1993.

Takahashi, T., Sutherland, S. C., Sweeney, C., Poisson, A., Metzl, N., Tilbrook, B., Bates, N., Wanninkhof, R., Feely, R. A., Sabine, C., Olafsson, J., and Nojiri, Y.: Global sea–air CO2 flux based on climatological surface ocean pCO2, and seasonal biological and temperature effects, Deep Sea Res. Part II Top. Stud. Oceanogr., 49, 1601–1622, https://doi.org/10.1016/S0967-0645(02)00003-6, 2002.

Tennekes, H.: The Logarithmic Wind Profile, J. Atmospheric Sci., 30, 234–238, https://doi.org/10.1175/1520-0469(1973)030<0234:TLWP>2.0.CO;2, 1973.

Vandemark, D., Salisbury, J. E., Hunt, C. W., Shellito, S. M., Irish, J. D., McGillis, W. R., Sabine, C. L., and Maenner, S. M.: Temporal and spatial dynamics of CO2 air-sea flux in the Gulf of Maine, J. Geophys. Res. Oceans, 116, https://doi.org/10.1029/2010JC006408, 2011.

Ward, N. D., Keil, R. G., Medeiros, P. M., Brito, D. C., Cunha, A. C., Dittmar, T., Yager, P. L., Krusche, A. V., and Richey, J. E.: Degradation of terrestrially derived macromolecules in the Amazon River, Nat. Geosci., 6, 530–533, 2013.

Ward, N. D., Krusche, A. V., Sawakuchi, H. O., Brito, D. C., Cunha, A. C., Moura, J. M. S., da Silva, R., Yager, P. L., Keil, R. G., and Richey, J. E.: The compositional evolution of dissolved and particulate organic matter along the lower Amazon River—Óbidos to the ocean, Mar. Chem., 177, 244–256, 2015.

Ward, N. D., Bianchi, T. S., Medeiros, P. M., Seidel, M., Richey, J. E., Keil, R. G., and Sawakuchi, H. O.: Where Carbon Goes When Water Flows: Carbon Cycling across the Aquatic Continuum, Front. Mar. Sci., 4, https://doi.org/10.3389/fmars.2017.00007, 2017.

Waters, J., Millero, F. J., and Woosley, R. J.: Corrigendum to "The free proton concentration scale for seawater pH", [MARCHE: 149 (2013) 8–22], Mar. Chem., 165, 66–67, https://doi.org/10.1016/j.marchem.2014.07.004, 2014.